JOURNAL OF VIROLOGY, May 1990, p. 2265–2279
0022-538X/90/052265-15$02.00/0

Vol. 64, No. 5

Assembly of *gag*-β-Galactosidase Proteins into Retrovirus Particles

THOMAS A. JONES, GABRIELLE BLAUG, MARK HANSEN, AND ERIC BARKLIS*

Vollum Institute for Advanced Biomedical Research and Department of Microbiology and Immunology, Oregon Health Sciences University, Portland, Oregon 97201

Received 19 October 1989/Accepted 28 December 1989

We studied the expression of β-galactosidase (β-gal) and 15 *gag*-β-gal fusion proteins in the presence of Moloney murine leukemia virus wild-type core (*gag*) proteins. Analysis indicated that proteins retaining the amino-terminal portion of *gag* through the capsid protein-coding region were incorporated into retrovirus particles. Proteins which deleted portions of the capsid protein were assembled into virions at low efficiency, indicating the importance of capsid protein interactions in retrovirus assembly. Fusion proteins which retained the amino-terminal matrix protein of the *gag* polyprotein but which lacked the capsid protein were released efficiently from cells in a nonviral form. The nonviral form was characterized by a high sedimentation coefficient and a low density, suggestive of membrane vesicles. While β-gal was present in the cytoplasm of expressing cells, all fusion constructs were associated with cellular membranes. *gag*-β-gal proteins which were capable of release from cells demonstrated a two-component immunofluorescence staining pattern consisting of a circle of fluorescence around the nucleus and a punctate pattern of staining throughout the remainder of the cell. Interestingly, fusions within the matrix protein were trapped intracellularly and yielded distinct perinuclear staining patterns, possibly localizing to the rough endoplasmic reticulum and/or Golgi. This observation suggests that Moloney murine leukemia virus *gag* proteins travel to the plasma membrane by vesicular transport associated with the cytoplasmic face of intracellular vesicles.

The process of retrovirus assembly requires that several viral components in an infected cell unite to form a mature virus particle. For all known avian, murine, and human retroviruses, infectious virions must include two copies of the viral genomic RNA with associated cellular tRNA primer; an envelope derived from the infected cell plasma membrane containing the protein products of the *env* gene; core proteins encoded by the viral *gag* gene; and enzymatic functions usually provided by *pol* gene products (58). The *gag* gene products appear to be central in the process of retrovirus assembly. Virion formation has not been observed in the absence of *gag* proteins, while assembly of (noninfectious) retrovirus particles occurs in the absence of *env* proteins (57), *pol* proteins (19), or the viral genome (27).

As with other retroviruses, the mechanism of Moloney murine leukemia virus (M-MuLV) assembly is poorly understood. Studies have shown that the *gag* gene products are translated initially as a 65-kilodalton precursor, $Pr65^{gag}$ (51, 61), which is proteolytically cleaved into the four M-MuLV *gag* proteins: MA is the amino-terminal matrix protein; p12 is the second protein, of unknown function; the major capsid protein, CA, is third from the amino terminus; and the nucleocapsid protein, NC, is a nucleic acid-binding protein and is located at the carboxy end of $Pr65^{gag}$ (3, 35). A convenient model for assembly of M-MuLV-type retroviruses, based on electron microscopic analysis, suggested the utility of encoding *gag* proteins in a polyprotein structure (6). By this model, the precursor protein is synthesized and targeted to the plasma membrane by determinants near the amino terminus of $Pr65^{gag}$, after which formation of the virus core, proteolytic cleavage, and virus budding occur. The model is attractive because it suggests mechanisms by which other viral constituents are incorporated into the particle; for instance, *env* proteins might be incorporated by specific binding to *gag* proteins at the cytoplasmic face of the plasma membrane; viral RNA could be drawn into the virion by its affinity to the NC protein at the carboxy terminus of $Pr65^{gag}$; and *pol* proteins, which are initially synthesized as a *gag-pol* fusion protein, would assemble into virions by virtue of their amino-terminal *gag* determinants.

Recent evidence supports at least one aspect of the above model. The amino termini of the M-MuLV and human immunodeficiency virus matrix proteins are modified by removal of initiator methionines and covalent attachment of the fatty acid myristate to the newly formed amino-terminal glycine residues (20, 56). Mutation of the glycine codons abolishes myristylation, eliminates *gag* protein-membrane association, and blocks virus assembly (41). Such results indicate that amino-terminal determinants of *gag* precursors are necessary for membrane association and virus assembly but do not delineate the protein regions which are sufficient for plasma membrane targeting. Also unresolved are details concerning the pathway of the *gag* precursors to the cell surface, the mechanism and site at which *gag* and *env* proteins associate, and the structural features essential for protein assembly into mature virions.

To delineate more completely the functional domains of the M-MuLV *gag* polyprotein and to examine the mechanism of *gag* protein assembly into virus particles, we developed a system for the analysis of *gag*-β-galactosidase (β-gal) proteins. For our studies, we constructed a series of gene fusions consisting of the β-gal-coding region fused to various portions of the 5′ coding region of the M-MuLV *gag* gene. The fusion proteins were expressed in the presence of wild-type proteins and analyzed with respect to their subcellular localization, release from cells to the medium, and incorporation into retrovirus particles. Our results clearly showed that fusion proteins containing M-MuLV MA, p12, and CA are efficiently incorporated into M-MuLV virions, while proteins containing deletions in the capsid protein are assembled into virus particles at lower efficiency. *gag*-β-gal fusion proteins containing fusions in the CA-coding region and several containing more extensive deletions were effi-

* Corresponding author.

ciently released from cells in what appeared to be membrane vesicles. Fusions which deleted a portion of the matrix protein appeared to be stuck in intracellular membrane compartments. These studies suggest that M-MuLV *gag* proteins are transported via membrane vesicles to the plasma membrane, where they may be released from cells in membrane vesicles or incorporated into budding retrovirus particles as a consequence of capsid protein interactions.

MATERIALS AND METHODS

Cell culture. NIH 3T3 fibroblast cells, Psi2 cells (32), and PA317 cells (33) were grown as described previously (4). Transfections were performed by the procedure of Graham and van der Eb (18) as modified by Parker and Stark (37). Infections of cells with virus were as described by Cepko et al. (8). Cell populations expressing BAG (39) or GBG constructs were generated by transfection of PA317 cells, infection of Psi2 cells with the PA317 culture supernatant collected 24 h after transfection, and selection of Psi2 cells with G418 as described previously (4). M-MuLV was from 3T3 cells which had been infected with a molecularly derived virus (40).

Recombinant plasmids. All recombinant retroviral constructs derive from the β-gal expression vector, BAG (39), which was generously provided by Connie Cepko. Plasmid constructs differ from BAG in the nonviral backbone region which is lost after infection of the Psi2 cells. All GBG constructs are identical to the BAG proviral portion except for the presence of variable portions of the M-MuLV 5′ *gag* coding region fused to the β-gal gene (see Fig. 1). Thus, GBG constructs represent a nested series of 3′ *gag* deletions fused to β-gal. For ease of construction, the *Bam*HI site at the 3′ side of the BAG β-gal gene was removed by partial *Bam*HI digestion, filling in of recessed ends, and ligation of the newly created blunt ends. Fusion of the β-gal gene was at a *Bam*HI site adjacent to codon 9 of β-gal. In BAG, the sequence at the β-gal junction is ATG GGC CCG GAT CCC GTC, in which the underlined A nucleotide (nt) is the first nt of the *gag* coding region at nt 621 of the M-MuLV genome (49) and the GTC codon is the ninth codon of β-gal. GBG numerical designations indicate the M-MuLV viral nucleotide positions (49) at which *gag* fusions occur. Some fusions were constructed utilizing specific restriction sites within the *gag* region by methodologies described Maniatis et al. (31). Other fusions were constructed at the endpoints of deletions generated by sequential use of exonuclease III and mung bean nuclease (21). The sequences at *gag*-β-gal junctions for the GBG constructs are as follows, in which the underlined nt marks the M-MuLV nt position designated in the GBG name and the final GTC codon represents the ninth codon of β-gal: GBG 648, TTA ACG GAT CCC GTC; GBG 730, GTT ACG GAT CCC GTC; GBG 917, CCC TTC GGA TCC GTC GAT CCC GTC; GBG 1035, GGC GAT ACC GTC GAT CCC; GBG 1174, CCT GCG GCG GAT CCC GTC; GBG 1198, TCC CCC GGA TCC GTC GAT CCC GTC; GBG 1224, CGG CGG ATC GAG GTC GAT CCC GTC; GBG 1363, GAA GAT CCG GAT CCC GTC; GBG 1486, TTA GAG GCG GAT CCC GTC; GBG 1560, CTC GAT CCC GTC; GBG 1698, GGG CCC CCC CTC GAG GTC GAT CCC GTC; GBG 1862, GAT TTG GGG GAT CCC GTC; GBG 2051, CTA TTG GCG GAT CCC GTC; GBG 2189, GGA CCT CGG CGG GAT CCC GTC; GBG 3705, GTC GAT CCC GTC.

Indirect immunofluorescence. Indirect immunofluorescence for β-gal and β-gal fusion proteins was performed by standard methods (16, 44). Briefly, cells grown on cover slips were fixed for 20 min in ice-cold phosphate-buffered saline (PBS) (9.5 mM sodium-potassium phosphate, 137 mM NaCl, 2.7 mM KCl, pH 7.4) containing 3.7% formaldehyde. Fixed cells were washed for 5 min at room temperature in PBS and then permeabilized at room temperature for 10 min in PBS plus 0.2% Triton X-100. Cells were then rinsed once with PBS and once with (Dulbecco modified Eagle medium plus penicillin, streptomycin, and 10% heat-treated calf serum) (DMEM/Calf). Each antibody incubation of 1 h at 37°C was followed by three 5- to 10-min DMEM/Calf washes at room temperature. The primary antibody was a 1:3,000 dilution of a mouse anti-β-gal antibody (Promgea Biotec, Madison, Wis.), and the secondary antibody was rhodamine-conjugated goat anti-mouse antibody (Tago) at a 1:100 dilution. After the last DMEM/Calf washes, cover slips were washed three times for 5 min each in PBS and mounted in 50% glycerol in PBS. Cells were viewed with a standard rhodamine filter.

Enzyme assays and cellular fractionation. Protein quantitation was by the method of Lowry et al. (30). β-gal assays were by the protocol of Norton and Coffin (34). Alkaline phosphodiesterase and 5′-nucleotidase assays were done by the procedures of Smith and Peters (50) and Widnell and Unkless (59), respectively. Reverse transcriptase assays were done by the procedure of Goff et al. (17), except that enzyme activity was quantitated by scintillation counting of labeled product. Crude subcellular fractionation was as described previously (11).

Sucrose density gradients and virus pelleting. Linear sucrose gradients (15 to 60% or 20 to 50%) were poured low density first from a Hoefer SG 100 gradient maker into the bottom of SW28 polyallomer tubes with 3-mm tubing. Gradients were 30 to 38 ml of sucrose in TSE (10 mM Tris hydrochloride, 100 mM NaCl, 1 mM EDTA, 0.1 mM phenylmethylsulfonyl fluoride). Either viral supernatant or the resuspended viral pellet from a 2- to 4-h 274,000 × *g* centrifugation was carefully layered on top of the gradient with a Pasteur pipette. The gradients were spun in an SW28 rotor for 4 to 71 h at 113,000 × *g* at +4°C. Fractions of 0.5 ml were bottom collected in microcentrifuge tubes with a Hoefer gradient fractionator. Samples were kept on ice after collection, mixed on a shaker for 1 to 3 min, and stored at −70°C for future assays. To show that the fusion proteins were at equilibrium in the gradient, 20 ml of viral supernatant from GBG 1560 expressing Psi2 cells was pelleted at 113,000 × *g* for 280 min and suspended in 520 μl of DMEM/Calf. One-half was loaded on the top of a 36-ml 15 to 60% gradient, and one-half was made 65% in 5 ml of TSE-sucrose and loaded onto the bottom of a similar gradient. Fractions were collected and assayed as above.

Labeling, immunoblotting, and immunoprecipitations. For protein gels, viral supernatant samples were spun for 2 h at 274,000 × *g* and 4°C and suspended in 100 to 200 μl of IPB (20 mM Tris hydrochloride [pH 7.5], 150 mM NaCl, 1 mM EDTA, 0.1% sodium dodecyl sulfate [SDS], 0.5% sodium deoxycholate, 1% Triton X-100, 0.02% sodium azide). Cells were washed twice with 10 ml of PBS (see above) and collected in 1 ml of IPB for 100-mm plates or 100 to 200 μl of IPB for 35-mm plates. Samples were prepared for loading by adding an equal volume of 2× sample buffer (12.5 mM Tris hydrochloride [pH 6.8], 2% SDS, 20% glycerol, 6.2 mg of dithiothreitol, per ml, 0.25% bromphenol blue) and 5% β-mercaptoethanol and boiling for 4 to 5 min. Samples were applied to SDS-polyacrylamide gels (Laemmli; 7.5 or 10%) and electrophoresed for 5 to 6 h at 35 mA. Proteins were

transferred onto 0.45-μm-pore-size nitrocellulose (Schleicher & Schuell, Inc., Keene, N.H.) with a Hoeffer TE52 electrophoresis unit in transfer buffer (25 mM Tris, 192 mM glycine, 20% methanol) for either 2 h at 500 mA or 15 h at 150 mA. The nitrocellulose was air dried for 30 min and stored in cling wrap at +4°C. Immunodetection of nitrocellulose-blotted proteins was done with alkaline phosphatase–anti-immunoglobulin G conjugates. All steps were done by rocking at room temperature. Membranes were wetted briefly in TBST (20 mM Tris hydrochloride [ph 7.6], 150 mM NaCl, 0.05% Tween 20) and then placed in 50 ml of 3% gelatin–TBST blocking solution for 30 min. This was replaced with 10 to 15 ml of a 1% gelatin–TBST primary antibody solution. For β-gal detection we used an anti-β-gal from mouse (Promega) at 1:7,500 dilution. An anti-M-MuLV polyclonal antibody from goat (81-S-107) was used to visualize viral proteins at a 1:1,500 dilution, and M-MuLV envelope proteins were visualized with anti-feline leukemia virus gP71 from goat at a 1:1,500 dilution. The membranes were washed three times for 10 min each with 50 ml TBST and rocked for 30 min in secondary antibody solutions of 1% gelatin–TBST and the appropriate anti-immunoglobulin G–alkaline phosphatase conjugate: antimouse for β-gal, anti-goat for 81-S-107, and anti-feline leukemia virus gP71. The membranes were again washed three times for 10 min each in 50 ml of TBST and then placed in 15 ml of a color reaction solution of 0.33 mg of Nitro Blue Tetrazolium, 0.17 mg of 5-bromo-4-chloro-3-indolyl phosphate, 100 mM Tris hydrochloride (pH 9.5), 100 mM NaCl, and 5 mM $MgCl_2$ until bands appeared. For myristic acid labeling experiments, [9,10-^{3}H]myristic acid (39.3 Ci/mmol; Dupont, NEN Research Products, Boston, Mass.) at 400 μCi/ml was used to label confluent monolayers of cells as described by Sefton et al. (47). Cell lysate samples were collected in 300 μl of IPB plus 0.1 mM phenylmethylsulfonyl fluoride and precleared by rocking at 4°C for 2 h with 80 μl of 10% protein A-Sepharose (Pharmacia, Inc., Piscataway, N.J.) in PBS, followed by microcentrifugation to remove protein A-Sepharose beads. Antibody incubations were performed by the addition of 800 μl of IPB plus phenylmethylsulfonyl fluoride plus a 1:5,000 dilution of mouse anti-β-gal (Promega) and by rocking the mixture overnight at 4°C. Antigen-antibody complexes were isolated by incubation for 1.5 h at 4°C with 80 μl of protein A-Sepharose beads. Beads washed five times were boiled for 4 to 5 min in 1× sample buffer plus 5% β-mercaptoethanol (see above), and eluted samples were electrophoresed as described above and fluorographed as described previously (26).

RESULTS

Release of *gag*-β-gal fusion proteins to the medium. To study the mechanism by which *gag* proteins become assembled into M-MuLV particles, we developed a system for the expression and analysis of *gag*-β-gal fusion proteins. Since *gag* proteins appear to be the only viral proteins required for assembly of retroviral particles (48), and since reverse transcriptase appears to be targeted to virions as a natural *gag-pol* fusion protein (15, 61), we reasoned the M-MuLV $Pr65^{gag}$ polyprotein would contain determinants sufficient to direct other *gag* fusion proteins into the virion assembly pathway. For our studies, we modified a β-gal expression vector (39) to express a series of *gag*-β-gal fusion genes containing various deletions of the *gag* carboxy-terminal coding region (Fig. 1A). These constructs, designated GBG plasmids, retain the same amino-terminal coding region of the *gag* polyprotein but differ in the extent of *gag* coding sequence fused to the β-gal gene. One (GBG 3705) contains the entire *gag* coding region as well as a portion of the *pol* gene fused to β-gal; two (GBG 2051 and 2189) are fused in the nucleocapsid-coding portion of gag; five are fused in the capsid region (GBG 1363, 1484, 1569, 1698, and 1862); four are fused in p12 (GBG 1035, 1174, 1198, and 1224); three (GBG 648, 730, and 917) are fused to the amino-terminal *gag* matrix protein; and the parental construct, BAG, contains two *gag* codons before the β-gal gene. The GBG plasmids also contain the selectable neomycin gene driven by the simian virus early promoter, permitting the selection of cells which are expressing the neomycin gene, followed by analysis of fusion protein expression in pooled resistant colonies. Constructs were transfected into the PA317 amphotropic packaging cell line, and PA317 supernatants were used to infect Psi2 cells (Fig. 1B). This method introduces proviral constructs into recipient cells by precise retrovirus integration rather than nonhomologous recombination, as seen in direct transfections. Unless otherwise indicated, fusion proteins were expressed in the presence of wild-type viral proteins in the Psi2 retrovirus-packaging cell line (32) to determine whether they could localize to regions where viral assembly occurs and interact with wild-type proteins to be incorporated into virions. This system permits analysis of signals involved in *gag* protein localization and incorporation into virions without requiring all aspects of *gag* protein function.

The initial characterization of fusion proteins involved quantitation of β-gal activity in Psi2 cells, which also express all the wild-type M-MuLV proteins. Total enzyme activity in matched samples of medium released from cells (supernatant) and in cell lysates was determined by standard procedures (34), and results are given (Table 1) as the ratio of the total activities in matched sets of samples. Note that normalization for total cellular protein and/or total reverse transcriptase activity in the supernatant yielded relative ratios similar to those shown. Also, since our assays were performed on concentrated supernatant material that had been pelleted at 274,000 × *g* for 2 to 4 h, activity associated with free protein would be selectively reduced in our samples relative to β-gal activity in high-molecular-weight structures or complexes.

As expected (Table 1), the amount of β-gal activity released from cells expressing the unfused enzyme in the BAG construct was very low, indicating that enzyme activity is not released by these cells in a readily sedimentable form. Direct assay of unpelleted supernatant from the BAG cells yielded no detectable β-gal activity (data not shown), indicating that unfused β-gal is also not measurably released from cells as a free protein. Even lower levels of β-gal activity were released to the medium in cells expressing β-gal fusions to deleted portions of the M-MuLV matrix protein. Constructs GBG 648, 730, and 917 expressed proteins containing 9, 37, and 99 codons, respectively, from the viral *gag* amino terminus; these fusion proteins were not released from cells. In contrast, all fusion proteins containing complete coding sequence for the matrix protein efficiently released β-gal activity to the medium. Generally, the two longest fusions efficiently released enzyme activity from cells, intermediate-length fusions released activity at a lower efficiency, and fusions in p12 released activity at an even lower efficiency. Nevertheless, all these *gag*-β-gal constructs released significantly higher levels of enzyme activity to the medium than did the control BAG construct. An additional point, to be discussed later, is that enzyme

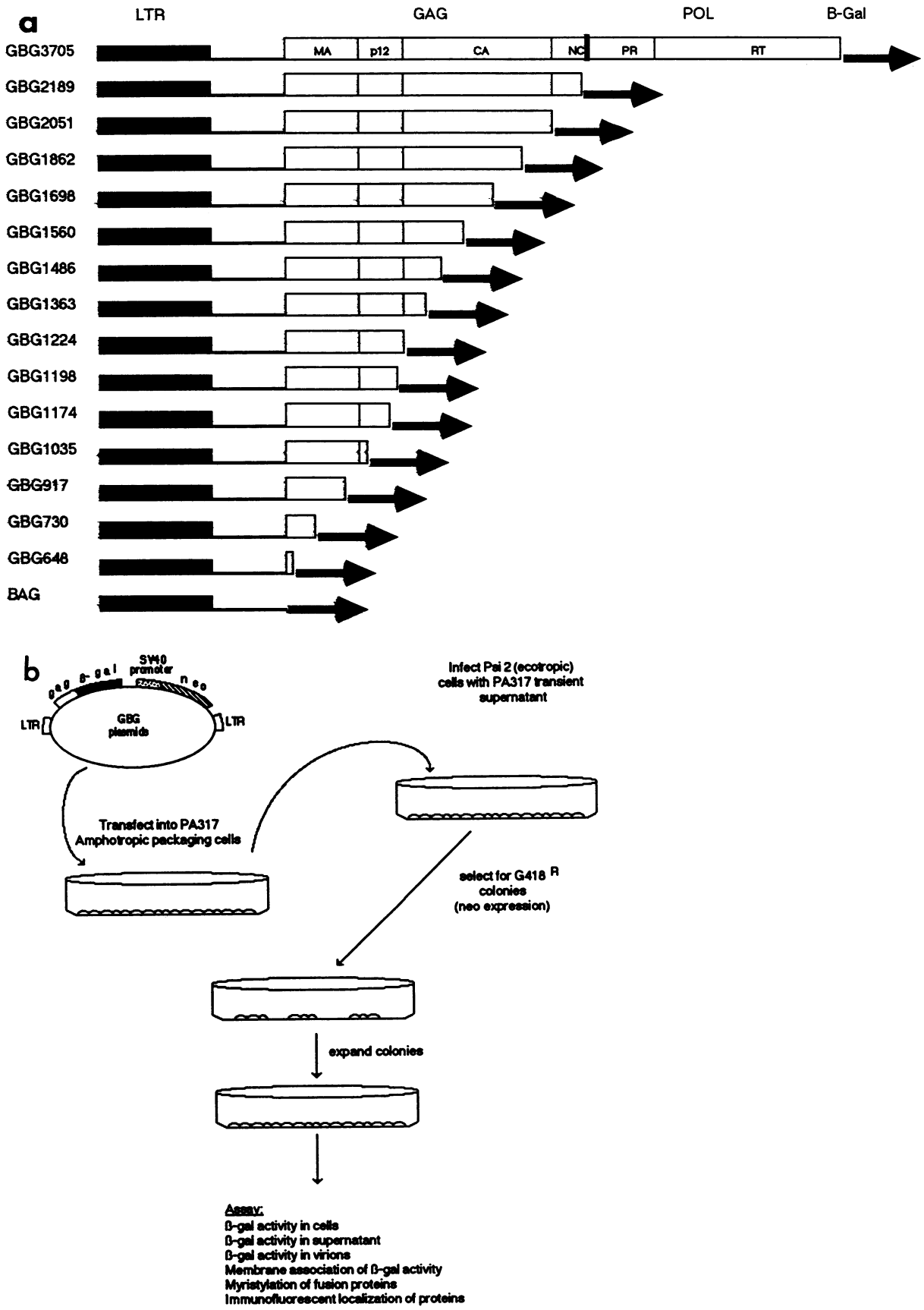
a
LTR
GAG
POL
B-Gal
MA
p12
CA
NC
PR
RT
GBG3705
GBG2189
GBG2051
GBG1862
GBG1698
GBG1560
GBG1486
GBG1363
GBG1224
GBG1198
GBG1174
GBG1035
GBG917
GBG730
GBG648
BAG
b
SV40 promoter
gag
β-gal
neo
LTR
GBG plasmids
LTR
Infect Psi 2 (ecotropic) cells with PA317 transient supernatant
Transfect into PA317 Amphotropic packaging cells
select for G418 R colonies (neo expression)
expand colonies
Assay:
β-gal activity in cells
β-gal activity in supernatant
β-gal activity in virions
Membrane association of β-gal activity
Myristylation of fusion proteins
Immunofluorescent localization of proteins

TABLE 1. β-Gal released from cells[a]

Construct (in Psi 2 cells unless indicated)	Supernatant/cell ratio (total β-gal supernatant/ total β-gal activity in cells)
BAG	0.017 ± 0.003
GBG 648	0.001 ± 0.000
GBG 730	0.004 ± 0.003
GBG 917	0.005 ± 0.004
GBG 1035	0.113 ± 0.020
GBG 1174	0.209 ± 0.011
GBG 1198	0.237 ± 0.128
GBG 1224	0.199 ± 0.065
GBG 1363	0.305 ± 0.142
GBG 1486	0.446 ± 0.206
GBG 1560	0.266 ± 0.040
GBG 1698	0.291 ± 0.004
GBG 1862	0.341 ± 0.001
GBG 2051	0.567 ± 0.127
GBG 2189	1.75 ± 0.170
GBG 3705	1.65
GBG 1560 (in 3T3 cells)	0.085 ± 0.016
GBG 1560 (in 3T3 cells infected with M-MuLV)	0.207 ± 0.002

[a] Psi2 cells (or 3T3 cells when indicated) expressing the indicated recombinant constructs were split 1:20 or 1:40 from confluence into 10-cm tissue culture plates and grown for 48 to 72 h. Supernatant medium (10 ml) was collected, filtered through a 0.45-μm-pore-size filter, pelleted at 4°C for 2 to 4 h at 274,000 × *g* (SW41 rotor at 40,000 rpm), and suspended in PBS before enzyme assay. Cells were washed twice with PBS, scraped from plates in 1 ml of PBS, in a microcentrifuge, and resuspended in PBS. Enzyme assays on aliquots of cell and supernatant samples were performed as described previously (34). From these aliquots, total cell and supernatant β-gal activities were calculated. Results are expressed as the ratio of total enzyme activity in the supernatant sample versus the cell sample, with standard deviations as indicated when possible. BAG values derived from 15 independent trials; GBG 1560 was from 9 trials; GBG 917, 1174, and 1198 were from 4 trials each; GBG 1224 and 1386 were from 3 experiments each; GBG 3705 was from 1 experiment; all other values derived from 2 experiments each.

activity was also released to the medium on expression of a fusion construct (GBG 1560) in 3T3 cells, which don't express wild-type viral proteins.

The results in Table 1 indicate that determinants in the matrix protein-coding region of the M-MuLV *gag* gene plus a small portion of the p12-coding region were sufficient to direct the release of fusion protein β-gal activity from Psi2 cells. While we assumed that β-gal enzyme activity accurately reflects fusion protein levels in cell supernatants and lysates, it was important to test this assumption. To do so, we subjected cell supernatant and lysate samples of cells expressing either free β-gal (BAG) or the GBG 1560 fusion protein to polyacrylamide gel electrophoresis, electroblotted proteins onto a nitrocellulose membrane, and immunodetected β-gal and β-gal fusion proteins as well M-MuLV envelope (*env*) proteins. Our results (Fig. 2) indicated that the M-MuLV envelope precursor protein ($Pr80^{env}$) is readily detected in Psi2 cells expressing either the BAG or GBG 1560 construct. Supernatants of each cell line contained the mature glycosylated *env* protein, gp70, and the ratios of cellular $Pr80^{env}$ to supernatant gp70 were roughly equivalent

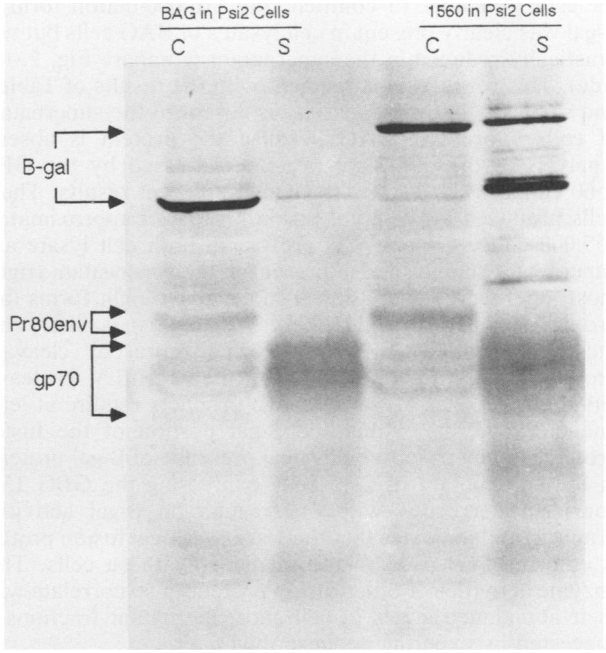

FIG. 2. β-Gal and envelope protein levels in cells and supernatants. Matched cell (C) and supernatant (S) samples were collected from Psi2 cells expressing either β-gal from the BAG construct or *gag*-β-gal from the GBG 1560 construct as described in the Materials and Methods. Cell samples (corresponding to 5% of the total cell sample) and supernatant samples (corresponding to 50% of the total sample) were subjected to SDS-polyacrylamide gel electrophoresis and electroblotted onto a nitrocellulose filter. β-Gal proteins were detected immunologically with a primary mouse anti-β-gal antibody, followed by a secondary alkaline phosphatase-conjugated goal anti-mouse antibody, followed by detection of alkaline phosphatase activity. Afterward, M-MuLV envelope proteins were detected by the same protocol but employing a primary goat anti-FeLV gp71 antibody and a phosphatase-conjugated rabbit antigoat secondary antibody. Lanes are as shown. Major β-gal-staining bands are indicated. The cellular M-MuLV envelope precursor protein, $Pr80^{env}$, is indicated, as is the characteristic wide band for the viral M-MuLV gp70.

FIG. 1. Recombinant constructs and methods. (A) All recombinant retroviral constructs derive from the β-gal expression vector, BAG (39), which expresses β-gal from the M-MuLV long terminal repeat (LTR) promoter by using the first two codons from the M-MuLV *gag* gene and also carries the neomycin gene expressed from the simian virus 40 (SV40) promoter for selection purposes. Proviral regions of *gag*-β-gal (GBG) constructs are identical to BAG except that the β-gal-coding region is fused to deletions of various lengths at the 3′ end of the M-MuLV *gag* gene. For most constructs, genes were fused employing *Bam*HI linkers (see Materials and Methods for specific details). GBG numerical designations indicate the M-MuLV viral nucleotide position (49) at which *gag* fusions occur. As illustrated, GBG 3705 contains the coding region for the entire *gag* gene as well as the *pol* gene protease (PR) and reverse transcriptase (RT) regions fused to β-gal; GBG 2051 and 2189 are fused in the nucleocapsid (NC)-coding portion of *gag*; GBG 1363 through 1862 are fused in the capsid (CA) region; GBG 1035 through 1224 are fused in p12; and GBG 648, 730, and 917 are fused in the matrix (MA)-coding region, generating fusion genes with 9, 37, and 99 codons, respectively, from the *gag* gene. (B) *gag*-β-gal fusion proteins were assayed as illustrated. Plasmids were transfected into the PA317 amphotropic packaging cell line to generate viral stocks for infection of the ecotropic packaging cell line Psi2, which produces all M-MuLV wild-type proteins as well as retrovirus particles. Infected Psi2 cells were selected for expression of the neomycin gene to isolate colonies of cells which had received the GBG (or BAG) provirus. Selected colonies were then pooled and expanded to yield Psi2 cells producing wild-type viral proteins as well as the β-gal or *gag*-β-gal fusion proteins. Expression of β-gal or fusion proteins was characterized as indicated.

for each cell line. In contrast, the 116,000-dalton form of β-gal was clearly present in cell lysates of BAG cells but was drastically reduced in the supernatant (compare Fig. 2, left side). This result is in agreement with the results of Table 1 and suggests that β-gal activity is absent in the supernatant of cells expressing BAG because the protein is absent. Analysis of the *gag*-β-gal protein expressed by the GBG 1560 construct in Psi2 cells yielded different results. These cells produced a *gag*-β-gal fusion protein of approximately 155,000 daltons which was present in both cell lysate and supernatant samples. Also present in the supernatant (rightmost lane) were several lower-molecular-weight forms (approximately 85,000 to 125,000). We think it is likely that these lower-molecular-weight forms represent cleavage products of the fusion protein by the M-MuLV protease, although the sizes of the cleavage products require at least one cleavage site within the β-gal portion of the fusion protein. In any case, the physical presence of β-gal proteins in the supernatant of Psi2 cells expressing the GBG 1560 construct correlates with our results on β-gal activities (Table 1) and indicates that the 1560 *gag*-β-gal fusion protein is efficiently released to the medium by these cells. That enzyme activities of other fusion proteins also correlate with their abundance levels in cell and supernatant fractions is suggested by experiments described later.

In addition to determination of protein levels in the cellular and supernatant fractions, other control experiments concerning the release of fusion proteins to the medium were also done. Supernatant enzyme activities of unfused β-gal and *gag*-β-gal fusions had similar half-lives (data not shown), indicating that the low β-gal level in the medium of cells expressing BAG was not due to degradation of supernatant protein. Intracellular enzyme activity per total protein in cells expressing a given construct remained constant over a variety of growth conditions (data not shown). The cell surface marker protein 5′-nucleotidase, as measured by a relatively insensitive colorimetric assay (59), was undetectable in cell supernatants, while plasma membrane marker protein alkaline phosphodiesterase, assayed with the substrate thymidine 5′-monophosphate-*p*-nitrophenyl ester (50), yielded a ratio of total supernatant to total cellular activity of 0.0245, similar to that seen for the BAG construct. These results suggest that the efficient release of *gag*-β-gal fusion proteins to the medium is not simply a consequence of random plasma membrane shedding from cells.

Association of fusion proteins with virus particles. Mature M-MuLV virions have a density in sucrose solutions of 1.15 to 1.18 g/ml (5) and contain reverse transcriptase activity. Free protein has a density of greater than 1.25 g/ml, and plasma membrane-derived vesicles have a density of 1.10 to 1.14 g/ml (2, 22). Therefore, to determine whether *gag*-β-gal fusion proteins were released to the medium in association with viral particles, we fractionated supernatant material on sucrose density gradients (15 to 60% or 20 to 50%) and assayed fractions for β-gal and reverse transcriptase activities (Fig. 3).

Performance of this experiment on medium from Psi2 cells expressing GBG 3705 (Fig. 3a) resulted in the appearance of overlapping peaks of β-gal and reverse transcriptase activities at a density of 1.15 g/ml. This result indicated that this fusion protein, which contains the entire *gag* coding region, is efficiently incorporated into virions. Interestingly, medium from cells expressing GBG 2051 (Fig. 3b) and 2189 (data not shown) contained two peaks of β-gal activity. One of these peaks, comprising 50 to 80% of the total β-gal activity, comigrated with the peak of reverse transcriptase activity and presumably represents fusion protein incorporated into virus particles. The second peak, which varied between 20 and 50% of the total supernatant β-gal activity for Psi2 cells expressing these clones, had a density of 1.11 to 1.14 g/ml and had no associated reverse transcriptase activity; we refer to this as the low-density fraction.

When medium from Psi2 cells expressing other *gag*-β-gal proteins was analyzed, we discovered that fusions of β-gal to the capsid protein-coding region (plasmids GBG 1363, 1486, 1560, 1698, and 1862) generated proteins which were largely excluded from virus particles. Of these proteins, 75 to 95% of the total supernatant β-gal activity was present in the low-density fraction, while 5 to 25% comigrated with the peak of reverse transcriptase activity (for example, see Fig. 3c). Similar examination of supernatant from cells expressing shorter fusion constructs (GBG 1035, 1174, 1198, and 1224) yielded only the low-density peak of β-gal activity (data not shown), although very low levels of enzyme activity associated with virus particles might not have been detected.

Is release of β-gal activity to the low-density fraction dependent on the presence of wild-type viral proteins? We addressed this question by expressing the GBG 1560 construct in uninfected 3T3 cells. As shown in Table 1, the amount of β-gal activity released to the medium in 3T3 cells expressing the GBG 1560 construct was fivefold higher than β-gal released by Psi2 cells producing free β-gal (supernatant-to-cell ratio of 0.085 versus 0.017). We examined the density of the β-gal activity released by the 3T3 cells (Fig. 3d) and found that all the GBG 1560 *gag*-β-gal enzyme activity released by 3T3 cells was in the low-density fraction. (No discernable peak of activity was identified when supernatant of cells producing free β-gal was subjected to density gradient centrifugation.) Upon superinfection of 3T3 cells expressing GBG 1560 with M-MuLV, an increase in released β-gal activity was detected (Table 1). Superinfected cells released, in addition to the low-density β-gal peak, a 1.18-g/ml density peak containing approximately 25% of the total enzyme activity overlapping with the peak of supernatant reverse transcriptase activity (Fig. 3e). These observations lead to two conclusions. First, the presence of the low-density β-gal activity in cell supernatants is independent of wild-type viral proteins. Second, the appearance of the high-density β-gal peak is a consequence of wild-type M-MuLV expression and probably reflects assembly of the *gag*-β-gal fusion protein into virus particles.

The exact nature of the β-gal-containing low-density supernatant fractions is unclear. Based on our ability to pellet this activity on short-duration centrifugations, we estimate the activity is present in a complex with a sedimentation coefficient of greater than 50 S (data not shown). Sucrose density gradient centrifugation of the low-density activity loaded at either the top or bottom of the gradient equilibrates at a density of 1.10 to 1.14 g/ml (data not shown). Complete enzyme activity requires detergent treatment of this fraction (data not shown). These observations are consistent with the notion that β-gal activity in the low-density fraction is contained within a lipoprotein complex, perhaps derived from plasma membrane vesicles.

Subcellular localization of fusion proteins. It was of interest to ascertain whether the subcellular localizations of the various *gag*-β-gal fusion proteins might help explain their relative efficiencies for release from cells to the supernatant. Therefore, we attempted to localize proteins by two methods: enzyme assay of crude subcellular fractions, and indirect immunofluorescence analysis. Our crude fractionation

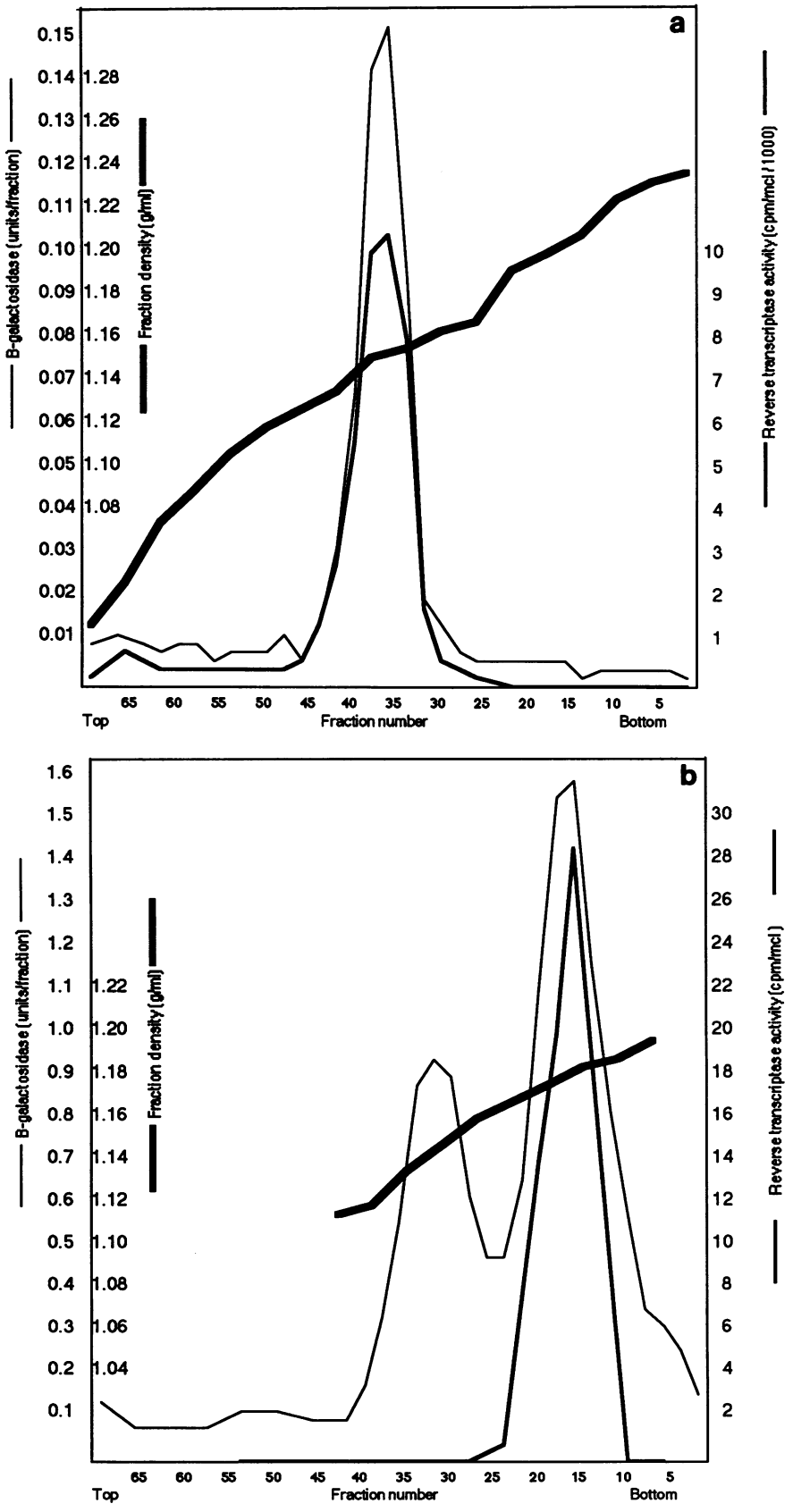
a
B-galactosidase (units/fraction)
Fraction density (g/ml)
Reverse transcriptase activity (cpm/mcl / 1000)
0.15
0.14
0.13
0.12
0.11
0.10
0.09
0.08
0.07
0.06
0.05
0.04
0.03
0.02
0.01
1.28
1.26
1.24
1.22
1.20
1.18
1.16
1.14
1.12
1.10
1.08
10
9
8
7
6
5
4
3
2
1
65 60 55 50 45 40 35 30 25 20 15 10 5
Top
Fraction number
Bottom
b
B-galactosidase (units/fraction)
Fraction density (g/ml)
Reverse transcriptase activity (cpm/mcl)
1.6
1.5
1.4
1.3
1.2
1.1
1.0
0.9
0.8
0.7
0.6
0.5
0.4
0.3
0.2
0.1
1.22
1.20
1.18
1.16
1.14
1.12
1.10
1.08
1.06
1.04
30
28
26
24
22
20
18
16
14
12
10
8
6
4
2
65 60 55 50 45 40 35 30 25 20 15 10 5
Top
Fraction number
Bottom

FIG. 3.

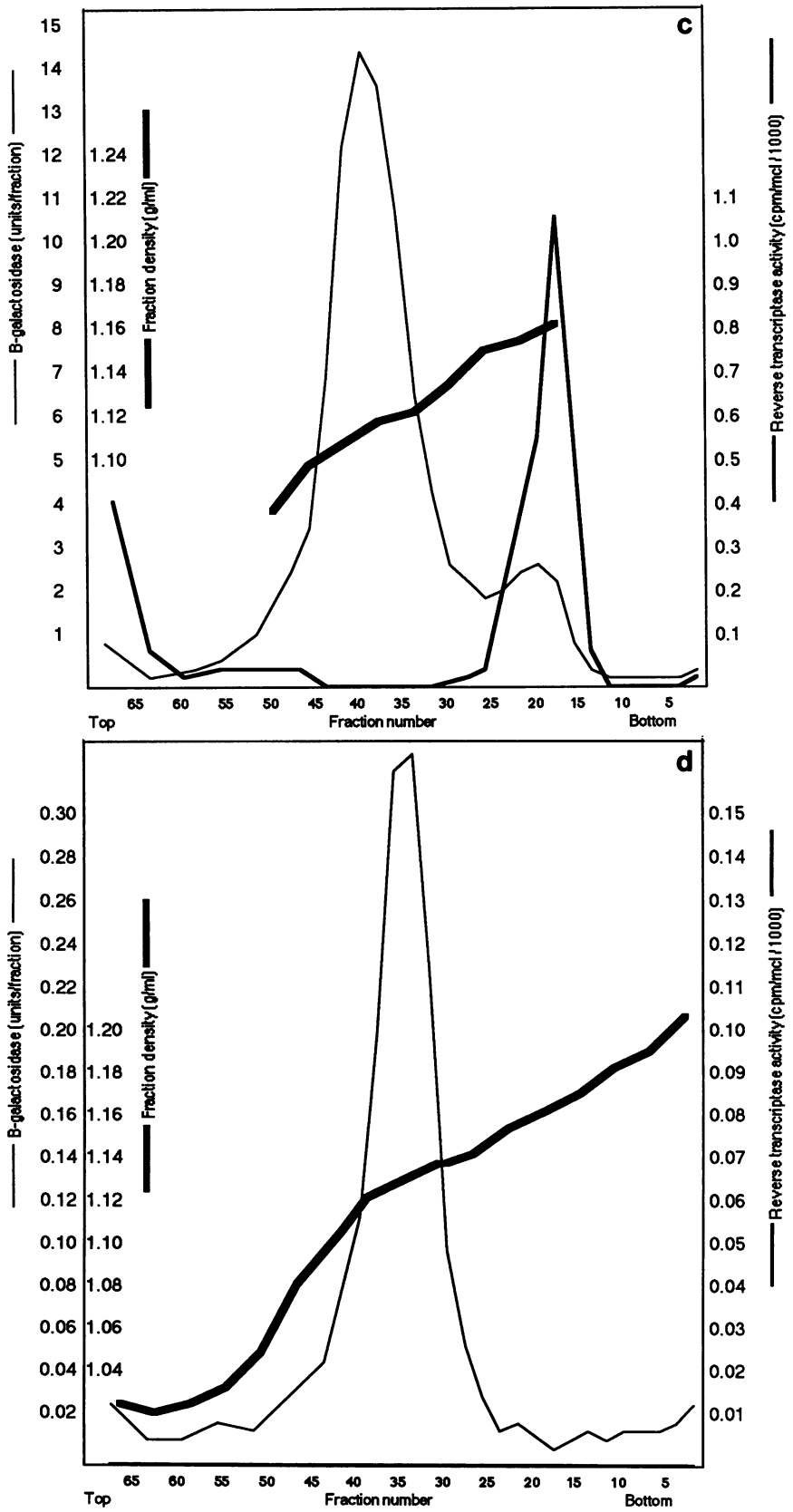

FIG. 3—*Continued.*

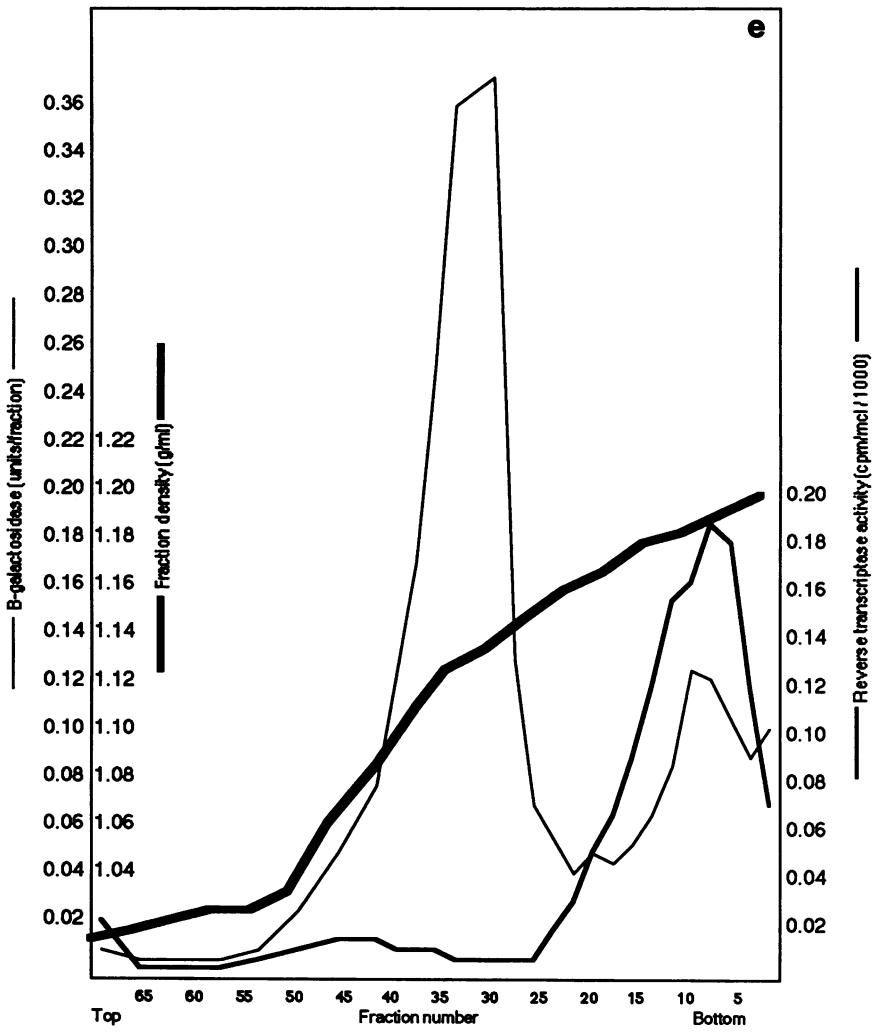

FIG. 3. Sucrose density gradient fractionation of supernatant material. Supernatant material from cells expressing the indicated constructs was fractionated by sucrose density gradient centrifugation as described in the Materials and Methods. Fractions of 0.5 ml were collected from the bottom of the gradients, and fraction densities, β-gal activities, and reverse transcriptase activities were determined. (a) A 15 to 60% gradient of supernatant material of GBG 3705 expressed in Psi2 cells. (b) A 20 to 50% gradient of GBG 2051 in Psi2 cells. (c) A 20 to 50% gradient of GBG 1363 in Psi2 cells. (d) A 15 to 60% gradient of GBG 1560 in 3T3 cells. (e) A 15 to 60% gradient of GBG 1560 expressed in 3T3 cells which were superinfected with M-MuLV.

procedure followed the standard protocol of Dickson and Atterwill (11) in which the nonuclear fraction of a cell lysate is separated into membrane (P2) and cytosolic (S2) fractions by high-speed centrifugation (Table 2). For each cell line expressing a β-gal construct, the ratio of membrane (P2) to cytosol (S2) enzyme activity, normalized for total protein, is listed. A low value reflects a cytosolic localization, while a high value indicates membrane association. As expected, the unfused β-gal produced by the BAG construct was distributed preferentially to the cytosolic fraction as represented by its low P2/S2 ratio. In contrast, all fusions containing at least 99 amino acids from the amino terminus of M-MuLV *gag* (constructs GBG 917 and larger) demonstrated at least a 50-fold greater specific activity in the membrane fraction. As indicated, in these cases greater than half of the S1 β-gal activity fractionated to membranes. Interestingly, our shortest fusions within the matrix protein, GBG 648 and 730, possessed low levels of membrane association. These fusion proteins had enzyme activity ratios 4 to 8 times higher than free β-gal, but 5 to 20 times lower than the longer fusion constructs.

To corroborate our results on the membrane association of the fusion proteins and to obtain additional information concerning their subcellular localizations, we analyzed β-gal and *gag*-β-gal proteins in fixed, permeabilized cells by indirect immunofluorescence, utilizing mouse anti-β-gal as a primary antibody and rhodamine-conjugated goat anti-mouse immunoglobulin G as the second antibody (Fig. 4). On Psi2 or 3T3 cells which do not express β-gal proteins, our procedure yielded a barely detectable haze of background fluorescence over the cells (data not shown). Similarly, exclusion of the primary antibody on cells expressing β-gal constructs resulted in only background fluorescence (data not shown). Examination of Psi2 cells expressing free β-gal from the BAG construct revealed an even distribution of protein throughout the cell (Fig. 4a). This staining pattern strongly suggests a cytoplasmic localization of the unfused β-gal, a conclusion which is supported by the results from

TABLE 2. Membrane association of fusion proteins[a]

Construct (in Psi2 cells unless indicated)	Total β-gal ratio (P2 β-gal/S2 β-gal)	Membrane association (β-gal P2/protein P2)/(β-gal S2/ Protein S2)
BAG	0.020 ± 0.012	0.116 ± 0.046
BAG (in 3T3 cells)	0.011	0.043
GBG 648	0.050	0.447
GBG 730	0.105 ± 0.078	0.862 ± 0.343
GBG 917	1.21 ± 0.940	5.86 ± 1.87
GBG 1035	13.1	17.05
GBG 1174	3.99 ± 3.93	9.11 ± 1.64
GBG 1198	1.59 ± 0.127	8.44 ± 1.23
GBG 1224	3.08	7.90
GBG 1363	1.60 ± 0.577	6.83 ± 1.75
GBG 1560	1.48 ± 0.683	5.53 ± 0.917
GBG 1560 (in 3T3 cells)	2.72 ± 0.900	8.22 ± 1.87
GBG 1698	6.32 ± 5.02	14.2 ± 1.09
GBG 1862	3.21 ± 2.96	5.78 ± 0.429
GBG 2051	9.17 ± 8.53	15.0 ± 3.30
GBG 2189	6.75 ± 3.86	11.2 ± 0.910

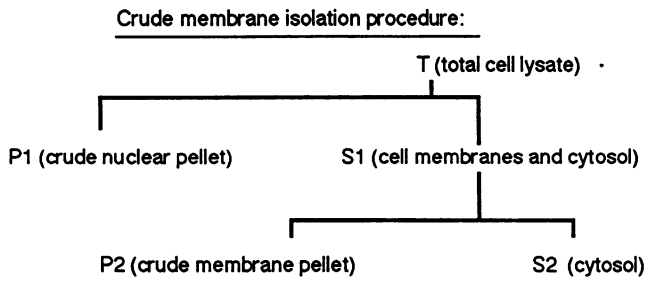

[a] Membrane association of proteins was monitored by crude cell fractionation (11) in a crude membrane fraction, P2, and a cytosolic fraction, S2. Proteins were expressed from the indicated constructs in Psi2 cells unless indicated. Fractions were assayed for β-gal activity (34) and protein (30). In the center column, ratios of total membrane (P2) versus cytosol (S2) activities are shown, along with standard deviations when possible. In the right-hand column, ratios of specific enzyme activities are given. BAG values derive from eight independent trails; GBG 1560 is from seven trials; GBG 1174 and GBG 1560 (in 3T3 cells) are from five trials each; GBG 917 values are from four experiments; GBG 730 and 1363 are from three experiments each; BAG (in 3T3 cells) and GBG 648, 1035, and 1224 values are each from one experiment; all other values derive from two experiments each.

Table 2. The immunofluorescence pattern observed on Psi2 cells expressing the intermediate-length fusion construct GBG 1560 was dramatically different (Fig. 4b). The *gag*-β-gal protein distribution in these cells appeared to have two components: a broad and intense perinuclear staining pattern and a punctate pattern of staining throughout the remainder of the cell, including numerous microvillue-type structures. The perinuclear component of this pattern is reminiscent of a rough endoplasmic reticulum-Golgi immunofluorescent staining pattern (29, 36), while the punctate pattern suggests staining of vesicles (43) perhaps associated with cytoskeleton. Whatever its derivation, this two-component staining pattern was observed in 3T3 cells expressing the GBG 1560 protein (Fig. 4c) and in Psi2 cells expressing the GBG 2051 protein (Fig. 4d). This pattern was obvious in all our examinations of cells expressing *gag*-β-gal fusions the length of GBG 1174 or longer, including GBG 1174, 1224, 1363, 1560, and 2051 (data not shown).

Surprisingly, the immunofluorescence patterns of the four shortest fusion proteins (GBG 648, 730, 917, and 1035) were distinct from the cytoplasmic pattern of the unfused β-gal and from the two-component pattern of the longer fusion proteins. GBG 1035 in Psi2 cells generated an immunofluorescence pattern in which the intensity of fluorescence in the punctate component was reduced somewhat relative to the perinuclear component (Fig. 4e). The localization pattern of the GBG 917 protein was different from that of any other protein in our study (Fig. 4f). Intense fluorescence was evident immediately adjacent to the nucleus in a nonhomogeneous ring; there was no fluorescence in the rest of the cell. Our shortest fusions, GBG 648 and 730, displayed similar patterns (Fig. 4g and h, respectively). The perinuclear patterns here were broad and pockmarked, and the remainder of the cell was dark. Close inspection at high magnification revealed pocks as small rings of fluorescence surrounding small unstained centers.

Our immunofluorescence studies, to a large extent, corroborated our experiments on release of fusion proteins to the medium and our membrane-cytosol fractionation studies. The unfused β-gal generated by the BAG construct was not released to the medium, fractionated to the cytosol, and appeared cytoplasmic on the basis of immunofluorescence analysis. Fusions which were released to the medium, proteins GBG 1035 and larger, were membrane associated and had the two-component fluorescence pattern of perinuclear plus punctate staining. As noted above, such proteins may or may not become incorporated into virions. *gag*-β-gal proteins which were not released to the medium are represented by the fusions of β-gal to the matrix-coding region of *gag* (GBG 648, 730, and 917). The GBG 917 protein had a high affinity with cellular membranes, as illustrated by our fractionation studies (Table 2), but the immunofluorescence pattern for this protein was solely perinuclear, lacking the punctate pattern of staining associated with the rest of the cell (Fig. 4f). The GBG 648 and 730 proteins were not released from cells, had a slight affinity to cellular membranes, and localized to a broad region surrounding the nucleus. The observed staining patterns for these proteins suggest that they are associated with intracellular membranes (Fig. 4g and h), although only a small percentage of each was retained in our P2 fraction (Table 2). This apparent discrepancy may be due to dissociation from membranes during fractionation.

Modifications of *gag*-β-gal proteins. There are at least two forms of murine retrovirus *gag* precursor proteins: the predominant $Pr65^{gag}$ protein, which is myristylated at its amino terminius (20), and a minor glycosylated *gag* protein, $gp85^{gag}$ (1, 12, 55), which is translated from an initiation codon 88 codons upstream from the $Pr65^{gag}$ AUG (38). Thus, all our constructs, which employ the wild-type M-MuLV sequence through the *gag* initiation codon, could be synthesized in myristylated and glycosylated forms. To determine whether β-gal proteins encoded by our constructs are glycosylated, we incubated BAG, GBG 1560, and GBG 2051 cells overnight in the presence or absence of 0.05 μg of tunicamycin per ml. These conditions are sufficient to prevent glycosylation of the envelope precursor protein $Pr80^{env}$ and render cells susceptible to viral superinfection (42). Tunicamycin treatment (Fig. 5a, lanes A, D, and F) caused the disappearance of $Pr80^{env}$ and the appearance of three incompletely glycosylated forms of the envelope protein (brackets). In contrast, patterns of β-gal and fusion protein expression were unaffected by tunicamycin treatment, suggesting that the major β-gal and *gag*-β-gal proteins of BAG- and GBG-expressing cells are unglycosylated. While we cannot exclude the possibility that a small proportion of our β-gal proteins are glycosylated, we estimate that such forms must constitute less than 10% of the total cellular β-gal

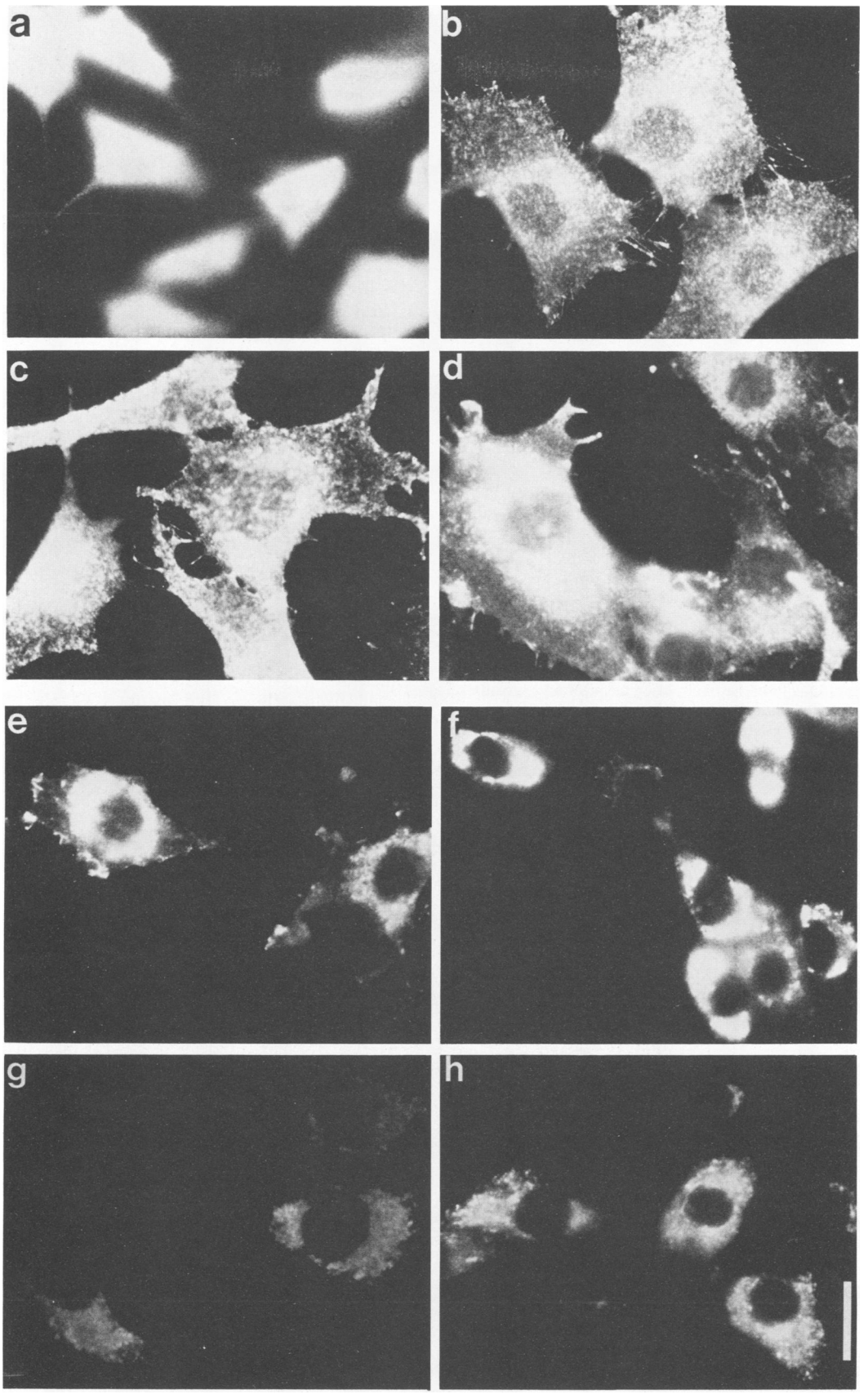

FIG. 4. Indirect immunofluorescence detection of β-gal and *gag*-β-gal fusion proteins in cells. Cells grown on cover slips were fixed, permeabilized, and subjected to indirect immunofluorescence analysis, utilizing mouse anti-β-gal antibody as the primary reagent, followed by rhodamine-conjugated goat antimouse antibody (see Materials and Methods). The white bar indicates 20 μm. All photographs are of proteins expressed in Psi2 cells unless otherwise indicated. (a) BAG; (b) GBG 1560; (c) GBG 1560 in 3T3 cells; (d) GBG 2051; (e) GBG 1035; (f) GBG 917; (g) GBG 730; (h) GBG 648.

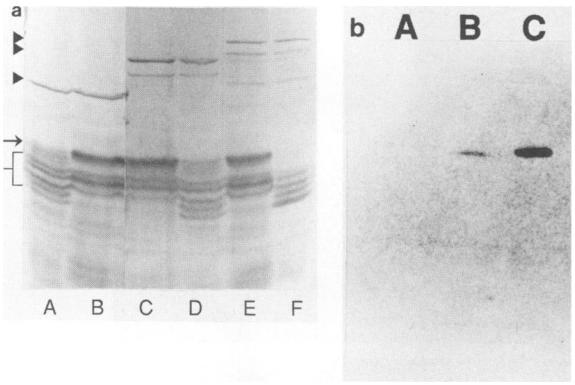

FIG. 5. (a) Effect of tunicamycin on β-gal and *gag*-β-gal proteins expressed in cells. BAG (lanes A and B), GBG 1560 (lanes C and D), and GBG 2051 (lanes E and F) cells were untreated (lanes B, C, and E) or treated for 19 h with 0.05 μg of tunicamycin per ml (lanes A, D, and F). β-Gal and M-MuLV proteins in cell lysates were then electrophoresed, electroblotted, and detected as described in the legend to Fig. 2. Triangles indicate the major cellular β-gal or *gag*-β-gal fusion proteins. $Pr80^{env}$ is indicated by the arrow; gp70 and the incompletely glycosylated envelope protein forms are marked by the bracket. (b) Myristylation of *gag*-β-gal proteins. Confluent 35-mm plates of Psi2 cells expressing BAG (lane A), GBG 648 (lane B), or GBG 730 (lane C) were labeled for 4 h with [^{3}H]myristic acid. After labeling, cells were lysed and β-gal or *gag*-β-gal proteins were immunoprecipitated. Precipitated proteins were subjected to SDS-polyacrylamide gel electrophoresis and detected fluorographically in the fixed, dried gel after an exposure of 21 days. The protein bands in lanes B and C migrate at approximately 120,000 daltons, as determined by comparison with known protein size markers.

protein in cells expressing the BAG and GBG constructs. If there are glycosylated versions of β-gal, we might expect that a small portion of the β-gal activity in our cell lines would act similarily to $gp85^{gag}$ with respect to its plasma membrane localization (12, 13) and its general exclusion from virions (14, 46, 55). However, since β-gal proteins expressed from the BAG construct were cytoplasmic (Table 2; Fig. 4) and since GBG 2051, 2189, and 3705 proteins were efficiently incorporated into virus particles (Table 1, Fig. 3), it appears that the contributions of putative glycosylated proteins in our studies are negligible.

Little or none of the β-gal protein expressed from our control construct BAG was expected to be myristylated; the BAG construct contains only the first two codons of $Pr65^{gag}$ and possesses a proline third residue, which blocks *gag* N-terminal myristylation (23). In contrast, proteins from all the GBG constructs, which retain a minimum of nine $Pr65^{gag}$ codons, should be myristylated, assuming a myristylation signal of six to seven amino-terminal residues (7, 24, 54). Since the GBG β-gal proteins were all membrane associated (Table 2; Fig. 4) and $Pr65^{gag}$ membrane association depends on myristylation (42), our localization studies indirectly suggest that the *gag*-β-gal proteins are myristylated. To test this assumption, cells expressing BAG and our two shortest fusion constructs, GBG 648 and 730, were labeled for 4 h in the presence of [^{3}H]myristic acid. After labeling, β-gal proteins were immunoprecipitated from cell lysates, subjected to polyacrylamide gel electrophoresis, and detected by fluorography (Fig. 5b). Although labeling by this protocol is characteristically inefficient and requires long exposure times (23, 41), myristylated *gag*-β-gal fusion proteins were clearly evident from cells expressing GBG 648 and 730 (Fig. 5b, lanes B and C). In contrast, the free cytoplasmic β-gal expressed from the BAG construct was not labeled with myristate (Fig. 5b, lane A). These results support previous studies concerning the signal for protein myristylation (7, 24, 54) and suggest that the *gag*-β-gal proteins expressed by the GBG constructs are myristylated.

DISCUSSION

We developed a system for characterization of M-MuLV *gag*-β-gal fusion proteins for analysis of the mechanism of retrovirus assembly. In this study, we focused on the release of proteins from cells, incorporation into virions, and the subcellular localizations of β-gal and 15 *gag*-β-gal fusion proteins. Since our fusion proteins were expressed predominantly in the presence of wild-type proteins, it was possible to analyze aspects of *gag* protein localization and assembly without regard to functional requirements at other stages of the viral life cycle.

Our parental construct, BAG (39), should produce an enzyme which is translated from the correct viral start site and employs the first two codons of the M-MuLV *gag* gene before the β-gal-coding sequence. The predicted amino-terminal sequence of this protein, MGPDPVLQPP, possesses proline as the third residue, which has been shown to block N-terminal myristylation (23). This protein, which we refer to as β-gal or unfused β-gal, did not appear to be myristylated (Fig. 5b) and served as a negative control in our experiments. Not surprisingly, unfused β-gal was not released from cells to the medium (Table 1; Fig. 2) and localized to the cytosol (Table 2; Fig. 4a). The cytoplasmic localization of this protein and its unaltered mobility in the presence of tunicamycin (Fig. 5a) indicated that putative glycosylated versions of β-gal did not contribute significantly to our studies.

In contrast to β-gal, the *gag*-β-gal fusion proteins appeared to be myristylated and membrane associated. Our shortest fusion protein, from the GBG 648 construct, had a predicted amino-terminal sequence of MGQTVTTPLTDPV, retaining the first nine codons of M-MuLV *gag*. Myristylation of this protein (Fig. 5b) was consistent with previous studies, identifying the initial six to seven amino acid residues of a protein as the myristylation signal (7, 24, 54). While different myristylated proteins may have different subcellular destinations (54), we were surprised by the patterns observed for our different *gag*-β-gal proteins. Specifically, the apparent association of the GBG 648 and 730 proteins with one form of intracellular membrane and of GBG 917 with another (Table 2; Fig. 4) was unexpected. The fluorescence patterns of these proteins appeared to represent subsets of the two-component pattern seen in cells expressing longer *gag*-β-gal fusion proteins (Fig. 4). It is possible that the localizations of these three fusions in the M-MuLV matrix protein reflect unnatural missortings of unnatural proteins. Alternatively, the GBG 648, 730, and 917 proteins may be blocked at various stages in the natural routing of viral *gag* proteins to the cell surface. We favor the latter explanation for several reasons. The localization patterns appear to represent a subset of the two-component pattern; the GBG 1035 pattern seems to represent a partially blocked protein; monensin treatment of GBG2051 cells generates fluorescence patterns similar to those of GBG648 and 730 cells (L. Jelinek and E. Barklis, unpublished observations); and our results are reminiscent of the intracellular trapping of altered and mutant transmembrane proteins (16, 25, 28, 44).

From our results (Table 1), it is clear that gene fusions containing all the M-MuLV matrix protein are released efficiently from cells, even in the absence of wild-type viral proteins. The *gag*-β-gal enzyme that was released from cells unassociated with virions was present in a complex with a low density (Fig. 3) and a high sedimentation coefficient and required detergent for complete activity. It is likely that these low-density complexes are plasma membrane-derived vesicles, although further characterization will be necessary to establish this point. At present, we do not know the mechanism by which fusion proteins are released to this low-density fraction, although at least three possibilities exist: fusion proteins may self-assemble into low-density viruslike particles, proteins may localize to cellular regions involved in export, or release of proteins may be a consequence of random shedding of plasma membranes to the medium. Since plasma membrane marker proteins 5′-nucleotidase and alkaline phosphodiesterase are not efficiently released from cells, we do not believe that random membrane shedding is a likely explanation. It is hoped that additional analysis of the low-density fraction will provide insight as to its origin.

As discussed above and as illustrated in Fig. 3, release of β-gal activity from cells does not correlate completely with incorporation into M-MuLV virions. Assuming that fusion protein levels are accurately reflected by β-gal activities in our sucrose gradients, these data suggest that assembly into virions requires an intact capsid protein. We did not observe β-gal activity associated with reverse transcriptase activity from constructs with complete deletions of the capsid protein. However, fusions within the capsid-coding region (GBG 1363, 1486, 1560, 1698, and 1862) were incorporated inefficiently into virions, while proteins retaining the entire capsid-coding region (GBG 2051, 2189, 3705) were assembled readily into retrovirus particles. On the basis of supernatant β-gal and reverse transcriptase activities, as well as estimates of 20 to 70 reverse transcriptase and 5,000 to 10,000 capsid A molecules per virion (58), we estimate that each virion produced by GBG 2051 cells contains at least 70 *gag*-β-gal molecules. Since this calculation is based on the specific activity of pure tetrameric β-gal, it almost certainly represents a minimal estimate for *gag*-β-gal proteins found in virions.

Our results on the incorporation of *gag*-β-gal proteins into M-MuLV particles suggest a model for the assembly of *gag* and *gag-pol* proteins into virions (Fig. 6). By this model, *gag* proteins are cotranslationally myristylated (10, 53, 60) and rapidly become associated with the external face of intracellular membranes. Myristylated *gag* proteins then may travel to the plasma membrane in association with the external face of membrane vesicles. Traffic of such vesicles may be to a specialized region of the plasma membrane and may be directed by components of the cytoskeleton. Our data suggest that the ability of proteins to travel this route would require an intact myristylated (41) matrix protein, although the carboxy terminus of the protein may be dispensable (9). After arrival at the plasma membrane, *gag* proteins may be released from cells in the low-density form or, depending on capsid protein interactions, may be assembled into a budding retrovirus particle. This model permits several explanations and makes several predictions with respect to retrovirus assembly. Targeting to the plasma membrane by vesicular traffic allows the matrix protein to associate with intracellular membranes, rather than requiring cytoplasmic travel before membrane association. Inhibition of vesicular transport would be expected to cause *gag* protein accumulation in intracellular membranes and could lead to the budding of virus into intracellular vesicles, as observed during some MuLV infections (45) and for *vpu* mutants of human immunodeficiency virus (52). Vesicular transport of *gag* proteins also suggests an intracellular association of *env* and *gag* proteins during biosynthesis. Finally, a requirement of the capsid-coding region for efficient incorporation into virions implies that the v-*abl*, v-*raf*, and Rs-*ras* *gag*-oncogene fusion proteins should not detected in viruses, since none of these proteins contains an intact capsid domain. We have begun to test the predictions above in our efforts to clarify the mechanism of retrovirus assembly.

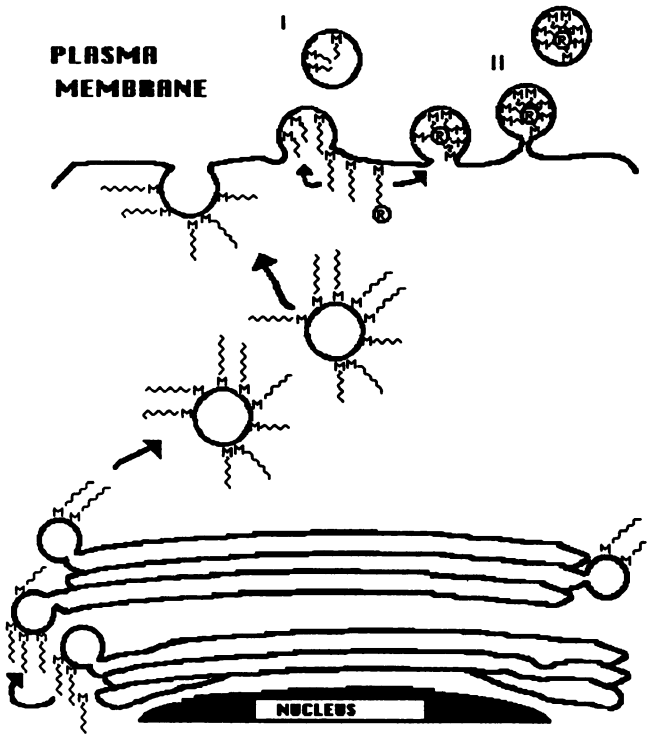

FIG. 6. Model of gag protein assembly into retrovirus particles. According to this model, the M-MuLV $Pr65^{gag}$ protein is cotranslationally myristylated and associates with the cytoplasmic face of intracellular membranes. Myristylated $Pr65^{gag}$ (indicated by the M and wavy line) travels to the plasma membrane by vesicular transport where it may be released in low-density vesicles (I) or into virus particles (II), depending on capsid protein interactions. Viral RNA (R) is assembled into virions by virtue of association with the carboxy terminus of $Pr65^{gag}$ and/or $Pr189^{gag\text{-}pol}$.

ACKNOWLEDGMENTS

We thank David Kabat, Harvey Lodish, Rudolf Jaenisch, and Scott Landfear for helpful discussions. The gift of the BAG construct from Connie Cepko is gratefully acknowledged. Richard Petersen and Jeffrey Comer provided excellent technical assistance.

This work was supported by grant 5-661 from the March of Dimes Birth Defects Foundation and by a grant (5R01 CA47088-02) from the National Cancer Institute.

LITERATURE CITED

1. **Arcement, L. J., W. I. Karshin, R. B. Naso, G. Jamjoom, and R. B. Arlinghaus.** 1976. Biosynthesis of Rauscher leukemia viral proteins: presence of p30 and envelope p15 sequences in precursor polypeptides. Virology **69**:763–774.
2. **Avruch, J., and D. F. H. Wallach.** 1971. Preparation and

properties of plasma membrane and endoplasmic reticulum fragments from isolated rat fat cells. Biochim. Biophys. Acta **233**:334–347.
3. **Barbacid, M., J. R. Stephenson, and S. A. Aaronson.** 1976. Gag gene of mammalian type-C RNA tumour viruses. (London) Nature **262**:554–559.
4. **Barklis, E., C. Mulligan, and R. Jaenisch.** 1986. Chromosomal position or virus mutation permits retrovirus expression in embryonal carcinoma cells. Cell **47**:391–399.
5. **Bolognesi, D. P., R. Luftig, and J. H. Shaper.** 1973. Localization of RNA tumor virus polypeptides. I. Isolation of further virus substructures. Virology **56**:549–564.
6. **Bolognesi, D. P., R. C. Montelaro, H. Frank, and W. Schafer.** 1978. Assembly of type C oncornaviruses: a model. Science **199**:183–186.
7. **Buss, J. E., C. J. Der, and P. A. Solski.** 1988. The six amino-terminal acids of $p60^{src}$ are sufficient to cause myristylation of $p21^{v\text{-}ras}$. Mol. Cell. Biol. **8**:3960–3963.
8. **Cepko, C., B. Roberts, and R. Mulligan.** 1984. Construction and applications of a highly transmissible murine retrovirus shuttle vector. Cell **37**:1053–1062.
9. **Crawford, S., and S. P. Goff.** 1984. Mutations in *gag* proteins P12 and P15 of Moloney murine leukemia virus block early stages of infection. J. Virol. **49**:909–917.
10. **Deichaite, I., L. P. Casson, H. Ling, and M. D. Resh.** 1988. In vitro synthesis of $pp60^{v\text{-}src}$: myristylation in a cell-free system. Mol. Cell. Biol. **8**:4295–4301.
11. **Dickson, C., and M. Atterwill.** 1980. Structure and processing of the mouse mammary tumor virus glycoprotein precursor Pr^{env}. J. Virol. **35**:349–361.
12. **Edwards, S. A., and H. Fan.** 1979. *gag*-related polyproteins of Moloney murine leukemia virus: evidence for independent synthesis of glycosylated and unglycosylated forms. J. Virol. **30**:551–563.
13. **Evans, L. H., S. Dresler, and D. Kabat.** 1977. Synthesis and glycosylation of polyprotein precursors to the internal core proteins of Friend murine leukemia virus. J. Virol. **24**:865–874.
14. **Fan, H., H. Chute, E. Chao, and M. Feuerman.** 1983. Construction and characterization of Moloney murine leukemia virus mutants unable to synthesize glycosylated gag polyprotein. Proc. Natl. Acad. Sci. USA **80**:5965–5969.
15. **Felsenstein, K. M., and S. P. Goff.** 1988. Expression of the *gag-pol* fusion protein of Moloney murine leukemia virus without *gag* protein does not induce virion formation or proteolytic processing. J. Virol. **62**:2179–2182.
16. **Gething, M., K. McCammon, and J. Sambrook.** 1986. Expression of wild-type and mutant forms of influenza hemagglutinin: the role of folding in intracellular transport. Cell **46**:939–950.
17. **Goff, S., P. Traktman, and D. Baltimore.** 1981. Isolation and properties of Moloney murine leukemia virus mutants: use of a rapid assay for release of virion reverse transcriptase. J. Virol. **38**:239–248.
18. **Graham, R., and A. van der Eb.** 1973. A new technique for the assay of infectivity of human adenovirus 5 DNA. Virology **52**:456–467.
19. **Hanafusa, H., D. Baltimore, D. Smoler, K. Watson, A. Yaniv, and S. Spiegelman.** 1972. Absence of polymerase protein in virions of alpha-type Rous sarcoma virus. Science **177**:1188–1191.
20. **Henderson, L. E., H. C. Krutzsch, and S. Oroszlan.** 1983. Myristyl amino-terminal acylation of murine retrovirus proteins: an unusual post-translational protein modification. Proc. Natl. Acad. Sci. USA **80**:339–343.
21. **Henikoff, S.** 1984. Unidirectional digestion with exonuclease III creates targeted breakpoints for DNA sequencing. Gene **28**: 351–359.
22. **Hubbard, A., D. Wall, and A. Ma.** 1983. Isolation of rat hepatocyte plasma membranes. I. Presence of the three major domains. J. Cell. Biol. **96**:217–229.
23. **Jorgensen, E., N. Kjeldgaard, F. Pedersen, and P. Jorgensen.** 1988. A nucleotide substitution in the *gag* N terminus of the endogenous ecotropic DBA/2 virus prevents $Pr65^{gag}$ myristylation and virus replication. J. Virol. **62**:3217–3223.
24. **Kaplan, J., G. Mardon, M. Bishop, and H. Varmus.** 1988. The first seven amino acids encoded by the v-*src* oncogene act as a myristylation signal: lysine 7 is a critical determinant. Mol. Cell. Biol. **8**:2435–2441.
25. **Kreis, T., and H. Lodish.** 1986. Oligomerization is essential for transport of vesicular stomatitis viral glycoprotein to the cell surface. Cell **46**:929–937.
26. **Laskey, R., and A. Mills.** 1975. Quantitative film detection of 3H and 14C in polyacrylamide gels by fluorography. Eur. J. Biochem. **56**:335–341.
27. **Levin, J., J. Grimley, J. Ramseur, and I. Berezesky.** 1974. Deficiency of 60 to 70S RNA in murine leukemia virus particles assembled in cells treated with actinomycin D. J. Virol. **14**: 152–161.
28. **Lippincott-Schwartz, J., L. Yuan, J. Bonifacino, and R. Klausner.** 1989. Rapid redistribution of Golgi proteins into the ER in cells treated with brefeldin A: evidence for membrane cycling from Golgi to ER. Cell **56**:801–813.
29. **Lipsky, N., and R. Pagano.** 1985. A vital stain for the Golgi apparatus. Science **228**:745–747.
30. **Lowry, O. H., N. J. Rosebrough, A. L. Farr, and R. J. Randall.** 1951. Protein measurement with the Folin phenol reagent. J. Biol. Chem. **193**:265–275.
31. **Maniatis, T., E. F. Fritsch, and J. Sambrook.** 1982. Molecular cloning: a laboratory manual. Cold Spring Harbor Laboratory, Cold Spring Harbor, N.Y.
32. **Mann, R., R. Mulligan, and D. Baltimore.** 1983. Construction of a retrovirus packaging mutant and its use to produce helper-free defective retrovirus. Cell **33**:153–159.
33. **Miller, A., and C. Buttimore.** 1986. Redesign of retrovirus packaging cell lines to avoid recombination leading to helper virus production. Mol. Cell. Biol. **6**:2895–2902.
34. **Norton, P., and J. Coffin.** 1985. Bacterial β-galactosidase as a marker of Rous sarcoma virus gene expression and replication. Mol. Cell. Biol. **5**:281–290.
35. **Oroszlan, S., L. Henderson, J. Stephenson, T. Copeland, C. Long, J. Ihle, and R. Gilden.** 1978. Amino- and carboxyl-terminal amino acid sequences of proteins coded by gag gene of murine leukemia virus. Proc. Natl. Acad. Sci. USA **75**:1404–1408.
36. **Pagano, R., and R. Sleight.** 1985. Defining lipid transport pathways in animal cells. Science **229**:1051–1057.
37. **Parker, B., and G. Stark.** 1979. Regulation of simian virus 40 transcription: sensitive analysis of the RNA species present early in infection by virus or viral DNA. J. Virol. **31**:360–369.
38. **Prats, A., G. De Billy, P. Wang, and J. Darlix.** 1989. CUG initiation codon used for the synthesis of a cell surface antigen coded by the murine leukemia virus. J. Mol. Biol. **205**:363–372.
39. **Price, J., D. Turner, and C. Cepko.** 1987. Lineage analysis in the vertebrate nervous system by retrovirus-mediated gene transfer. Proc. Natl. Acad. Sci. USA **84**:156–160.
40. **Reik, W., H. Weiher, and R. Jaenisch.** 1985. Replication-competent Moloney murine leukemia virus carrying a bacterial suppressor tRNA gene: selective cloning of proviral and flanking host sequences. Proc. Natl. Acad. Sci. USA **82**:1141–1145.
41. **Rein, A., M. McClure, N. Rice, R. Luftig, and A. Schultz.** 1986. Myristylation site in $Pr65^{gag}$ is essential for virus particle formation by Moloney murine leukemia virus. Proc. Natl. Acad. Sci. USA **83**:7246–7250.
42. **Rein, A., A. Schultz, J. Bader, and R. Bassin.** 1982. Inhibitors of glycosylation reverse retroviral interference. Virology **119**:185–192.
43. **Rindler, M., I. Ivanov, and D. Sabatini.** 1987. Microtubule-acting drugs lead to the nonpolarized delivery of the influenza hemagglutinin to the cell surface of polarized Madin-Darby canine kidney cells. J. Cell. Biol. **104**:231–241.
44. **Rose, J., and J. Bergmann.** 1983. Altered cytoplasmic domains affect intracellular transport of the vesicular stomatitis virus glycoprotein. Cell **34**:513–524.
45. **Roth, M., R. Srinivas, and R. Compans.** 1983. Basolateral maturation of retroviruses in polarized epithelial cells. J. Virol. **45**:1065–1073.
46. **Schwartzberg, P., J. Colicelli, and S. Goff.** 1983. Deletion

mutants of Moloney leukemia virus which lack glycosylated *gag* protein are replication competent. J. Virol. **46**:538–546.
47. **Sefton, B., I. Trowbridge, J. Cooper, and E. Scolnick.** 1982. The transforming proteins of Rous sarcoma virus, Harvey sarcoma virus and Abelson virus contain tightly bound lipid. Cell **31**: 465–474.
48. **Shields, A., O. Witte, E. Rothenberg, and D. Baltimore.** 1978. High frequency of aberrant expression of Moloney murine leukemia virus in clonal infections. Cell **14**:601–609.
49. **Shinnick, T., R. Lerner, and J. Sutcliffe.** 1981. Nucleotide sequence of Moloney murine leukemia virus. Nature (London) **293**:543–548.
50. **Smith, G., and T. Peters.** 1980. Analytical subcellular fractionation of rat liver with special reference to the localization of putative plasma membrane marker enzymes. Eur. J. Biochem. **104**:305–311.
51. **Stephenson, J., S. Tronick, and S. Aaronson.** 1975. Murine leukemia virus mutants with temperature-sensitive defects in precursor polypeptide cleavage. Cell **6**:543–548.
52. **Strebel, K., T. Klimkait, and M. Martin.** 1988. A novel gene of HIV-1, vpu, and its 16-kilodalton product. Science **241**:1221–1223.
53. **Towler, D., S. Eubanks, D. Towery, S. Adams, and L. Glaser.** 1987. Amino-terminal processing of proteins by N-myristoylation. J. Biol. Chem. **262**:1030–1036.
54. **Towler, D., J. Gordon, S. Adams, and L. Glaser.** 1988. The biology and enzymology of eukaryotic protein acylation. Annu. Rev. Biochem. **57**:69–99.
55. **Tung, J., T. Yoshiki, and E. Fleissner.** 1976. A core polyprotein of murine leukemia virus on the surface of mouse leukemia cells. Cell **9**:573–578.
56. **Veronese, F. M., T. D. Copeland, S. Oroszlan, R. C. Gallo, and M. G. Sarngadharan.** 1988. Biochemical and immunological analysis of human immunodeficiency virus *gag* gene products p17 and p24. J. Virol. **62**:795–801.
57. **Weiss, R.** 1969. Interference and neutralization studies with Bryan strain Rous sarcoma virus synthesized in the absence of helper virus. J. Gen. Virol. **5**:529–539.
58. **Weiss, R., N. Teich, H. Varmus, and J. Coffin (ed.).** 1984. RNA tumor viruses, 2nd ed. Cold Spring Harbor Laboratory, Cold Spring Harbor, N.Y.
59. **Widnell, C., and J. Unkless.** 1968. Partial purification of a lipoprotein with 5′-nucleotidase activity from membranes of rat liver cells. Proc. Natl. Acad. Sci. USA **61**:1050–1057.
60. **Wilcox, C., J. Hu, and E. Olson.** 1987. Acylation of proteins with myristic acid occurs cotranslationally. Science **238**:1275–1278.
61. **Witte, O., and D. Baltimore.** 1978. Relationship of retrovirus polyprotein cleavages to virion maturation studied with temperature-sensitive leukemia mutants. J. Virol. **26**:750–761.